De Novo Design, Synthesis, and Characterization of a Pore-Forming Small Globular Protein and Its Insertion into Lipid Bilayers†

Sannamu Lee,*,‡ Taira Kiyota,‡ Takahiro Kunitake,‡ Eiji Matsumoto,‡ Shoji Yamashita,§ Kazunori Anzai,|| and Gohsuke Sugihara‡

Department of Chemistry, Faculty of Science, Fukuoka University, Jonan-ku, Fukuoka 814-80, Japan, Department of Forestry, Faculty of Agriculture, Kyushu University, Higashi-ku, Fukuoka 812, Japan, and National Institute of Radiological Sciences, Anagawa, Inage-ku, Chiba 263, Japan

Received September 29, 1996; Revised Manuscript Received January 6, 1997⊗

ABSTRACT: The question of how to design a water-soluble globular protein remains. We report here the synthesis of a native-like and pore-forming small globular protein (SGP, 69 amino acid residues). The protein was designed to have four helices: a Trp-containing short hydrophobic helix in the middle surrounded by three Tyr-containing long basic amphiphilic helices. Size-exclusion chromatography and CD measurements indicated that in buffer solution SGP is monomeric with a 50% helical structure. SGP did not completely denature even at high temperature (90 °C) and at relatively high Gu·HCl concentration so that the denaturant concentration at the midpoint of the transition is 5 M. Dye binding studies and fluorescence energy transfer experiments showed that SGP possesses a hydrophobic binding site and its Trp of the central helix is present at a relatively hydrophobic region and accepts the energy from Tyr(s) in other amphiphilic helices, indicating that SGP takes a stable globular-like structure in aqueous solution. From the depth-dependent fluorescent studies using egg PC liposomes containing *n*-doxyl fatty acids and brominated phospholipid as quenchers, it was found that the hydrophobic central α-helix is able to enter spontaneously into the lipid bilayers and the Trp in the central α-helix is located at about the middle of the alkyl chain in the outer layer of the phospholipid bilayer. The peptide is also able to increase the membrane permeability with two modes of current (basal current and single ion channel) in planar phospholipid bilayers, indicating the spontaneous insertion of the protein into the lipid bilayer (basal current) and then the formation of a uniform size of channel pore (14 pS). SGP is useful as a basic and starting model to find good amino acid sequences that fold to a desired protein structure and to search translocation mechanisms from aqueous solution into lipid bilayers.

To better understand the insertion of membrane targeting protein into biomembrane, we designed and synthesized a small globular protein (SGP) and studied the folding structure in aqueous solution as well as the actual penetration mechanism into lipid bilayers. Colicins, water-soluble toxic proteins (Konisky, 1982), have been investigated in order to understand how this enters spontaneously into a nonpolar membrane environment (van der Goot et al., 1991; Mel et al., 1993). The C-terminal of colicin A is a folding structure composed of 10 α-helices, 2 of them forming a hydrophobic helical hairpin buried in the soluble protein (Parker et al., 1989). In the first phase of membrane penetration, the protein unfolds into a flexible conformation, the so-called molten globular state. The molten globular structure lowers the energy required for the hydrophobic hairpin to slip in, leaving an opened umbrella-like structure.

This insertion mechanism appears common to all pore-forming colicins. However, the picture of protein translocation and pore formation is not complete yet, because good model systems to obtain details of the mechanism of lipid bilayer insertion are not available. Thus, the *de novo* synthesis of artificial protein, SGP, was used to see if this translocation mechanism occurs in other membrane targeting proteins.

De novo synthesis of artificial protein has been an emerging area of research that not only tests our understanding of protein structure related to folding but also plays a role as the groundwork for the macromolecules with unprecedented structures and properties [see review by Bryson et al. (1995)]. Self-assembly or simultaneous folding is essential in *de novo* design of proteins. The propensity of amphiphilic peptides to assemble in aqueous solution and of the β-turn to form a loop has been successfully employed to design a coiled-coil protein and a 4,5,6-helix bundle protein (Regan & DeGrado, 1988; DeGrado et al., 1989; Hecht et al., 1990; Dekker et al., 1993; Zhou et al., 1992; Kamtekar et al., 1993; Monera et al., 1996), β-structural protein (Quinn et al., 1994), and metalloprotein (Handel et al., 1993). However, a protein with a buried hydrophobic helix similar to colicins has not been designed yet. We report here a native-like small globular protein (SGP) which is expected to fold as shown in Figure 1. The protein designed and synthesized has 4 helices with a short hydrophobic helix and 3 long basic amphiphilic helices in 69 amino acid residues, and is expected to spontaneously insert itself into membrane (Figure 1C). In the present study, we investigated the solution behavior of SGP and its insertion from aqueous solution to lipid bilayers.

† This work was supported in part by a Grant-in Aid for Scientific Research (C), Ministry of Education, Culture, and Science of Japan, and from the Central Institute of Fukuoka University and by a grant of the Science Promotion Foundation of Kim Man-Yu.

* To whom correspondence should be addressed.
‡ Fukuoka University.
§ Kyushu University.
|| National Institute of Radiological Sciences.

⊗ Abstract published in *Advance ACS Abstracts,* March 1, 1997.

S0006-2960(96)02451-8 CCC: $14.00

MATERIALS AND METHODS

Peptide Synthesis. SGP was synthesized according to the Fmoc[1] chemical procedure starting from Fmoc-Leu-PEG [poly(ethylene glycol)] resin by using a Miligen automatic peptide synthesizer (Model 9050) to monitor the deprotection of the Fmoc group by the UV absorbance. After cleavage from the resin by trifluoroacetic acid, the crude peptide obtained was purified by HPLC chromatography with an ODS column, 20 × 250 mm, with a gradient system of water/acetonitrile containing 0.1% trifluoroacetic acid. Amino acid analysis was performed after hydrolysis in 5.7 M HCl in a sealed tube at 110 °C for 24 h. Analytical data obtained were as follows: Gly, 6.2 (6); Ala, 9.5 (10); Leu, 26.5 (25); Asp, 3.0 (3); Pro, 2.9 (3); Tyr, 3.1 (3); Lys, 18.9 (18). Molecular weight was determined by the FAB-mass spectrum using a JEOL JMX-HX100: base peak, 7555.1; calcd for $C_{367}H_{639}O_{77}N_{91}{\cdot}H^+$, 7554.8. Peptide concentrations were determined from the UV absorbance of Trp and three tyrosines at 280 nm in buffer ($\epsilon = 8000$). Gel filtration HPLC chromatography was performed by using Tris buffer (10 mM Tris, 150 mM NaCl, pH 5.0 or pH 7.4) on COSMOSIL 5DIOL-300 (Nakalai Tesk, Kyoto, Japan).

Liposome Preparation. Small unilamellar egg PC liposomes were prepared as follows: egg PC (4.4 mg, about 6.0 μmol) in chloroform (2 mL) was placed in a round-bottom flask. After evaporation of the solvent, residual film was dried *in vacuo* overnight. The lipid film was hydrated with 3 mL of Tes buffer (5 mM Tes/100 mM NaCl, pH 7.4). The suspension was vortexed for 20 min. The turbid solution was sonicated under ice-cooling and nitrogen-flowing for 10 min (×3) by using a titanium tip sonicater. The liposome solution was centrifuged at 5000 rpm for 20 min.

CD Spectrum Measurements. CD spectra were recorded in Tes buffer (5 mM Tes/100 mM NaCl, pH 7.4) on a Jasco J-600 spectropolarimeter using a quartz cell of 1 mm path length. Peptide concentration was held at about 10 μM. CD values are expressed as the mean residue molar ellipticity. The percent helix was estimated using the equation: $\theta_{222} = (f_h - i\kappa/N)(\theta_{h,\,222\infty})$ where θ_{222} is the mean residue molar ellipticity at 222 nm; f_h, the fraction in α-helical form; i, the number of helices (assumed to be four); κ, a wavelength-specific constant with a value of 2.6 at 222 nm; N, the number of residues in the peptide (69 residues); and $(\theta_{h,\,222\infty})$, the molar ellipticity for an infinite chain length at 222 nm (−39 500 deg·cm^2/dmol) (Chen et al., 1974; Chang et al., 1978).

For the denaturation study, the stock solution of SGP made up using Tes buffer (5 mM Tes/100 mM NaCl, pH 7.4) was diluted to 10 μM by adding an appropriate quantity of 8 M Gu·HCl/Tes buffer solution. After the solution was left to stand for 1 h, the spectra were taken at 25 °C.

Fluorescence Measurement. All steady-state fluorescence measurements were performed with a Hitachi 850 fluorescence spectrophotometer. The fluorescence spectra were taken with excitation and emission band-passes of 5 nm. Correction was made for the contribution from the blank and the wavelength dependence of the instrumental response. Quenching of Trp fluorescence by acrylamide was performed in Tes buffer in the presence and absence of 200 μM egg PC liposomes. After peptides (4.4 μM) were added to the preformed small unilamellar liposomes, aliquots of 1 M acrylamide solution in buffer were added. The quenching data were analyzed by the Stern−Volmer plot using the equation, $F_0/F = 1 + K_{sv}[Q]$, where F_0, F, K_{sv}, and [Q] are the fluorescence intensities at maximum wavelength in the absence and presence of liposomes, the Stern−Volmer quenching constant, and the quencher concentration, respectively. Quenching experiments by *n*-doxylstearic acids were also performed as described above except for the titration study, in which the peptide solution was titrated with the liposome solution allowed to incorporate quenchers to the preformed liposome solution. The quenching of Trp fluorescence by lipid bilayers containing 1,2-bis(9,10-dibromostearoyl)phosphatidylcholine (DBRPC) as a quencher (Dawidowicz & Rothman, 1976) was also performed in Tes buffer. Peptide was titrated with liposome solution prepared from a mixture of the appropriate ratio of egg PC and DBRPC as described above.

Fluorescence Decay Measurements. These were performed using the multiwavelength time-resolved photon counting system (Type C4708, Hamamatsu). This system was constructed mainly with a combination of monochromator and streakscope that enables multiwavelength time-resolved photon counting with high speed (time resolution, 5 ps) and high sensibility. The excitation pulse was obtained from a mode-locked Ti:sapphire laser pumped by an argon ion laser (type 2080). In order to set the excitation wavelength at 285 nm, a third harmonics generator (GW-3FS, Spectra Physics) was used. Finally, output laser pulses for excitation have a pulse width narrower than 100 fs, and its repetition was 80 MHz. Fluorescence decay data were analyzed with a nonlinear least-squares algorithm (McKinnon et al., 1977). Adequacy of fluorescence was judged by inspection of plots of weighted residual and statistical parameters such as a reduced chi (χ) square.

Channel Formation Measurements. A planar lipid bilayer membrane was formed to the portion of an apparatus of about 200 μm in diameter on a Teflon septum between two compartments (cis for the compartment to which samples are added and trans for the opposite compartment) by folding of monolayers in a buffer containing 150 mM or 1 M KCl and 10 mM Tris−Hepes (pH 7.4) as described previously (Agawa et al., 1991). The 2:1 mixture of egg PC (Avanti Polar Lipids) and brain phosphatidylserine (Avanti Polar Lipids) was used as the bilayer lipid. In some experiments, after formation of the bilayer with 150 mM KCl and 10 mM Tris−Hepes (pH 7.4), the KCl concentration at the cis compartment was increased by withdrawing an appropriate volume of the cis solution followed by adding the same volume of 3 M KCl and 10 mM Tris−Hepes (pH 7.4). The SGP peptides dissolved in methanol or in a 150 mM KCl and 10 mM Tris−Hepes buffer solution (pH 7.4) were added to the cis compartment with stirring under voltage clamp conditions. The membrane potential was defined as the potential of the cis with respect to the trans compartment.

[1] Abbreviations: ANS, 1-anilinonaphthalene-8-sulfonate; CD, circular dichroism; DBRPC, 1,2-bis(9,10-dibromostearoyl)phosphatidylcholine; egg PC, egg yolk phosphatidylcholine; egg PE, egg yolk phosphatidylethanolamine; brain PS, bovine brain phosphatidylserine; Fmoc, 9-fluorenylmethoxycarbonyl; Gu·HCl, guanidine hydrochloride; HPLC, high-performance liquid chromatography; *n*-DS, *n*-doxylstearic acid; Hepes, 4-(2-hydroxyethyl)-1-piperazineethanesulfonic acid; Tes, *N*-[tris(hydroxymethyl)methyl]-2-aminoethanesulfonic acid; Tris, tris(hydroxymethyl)aminomethane. All amino acids are of the L-configuration.

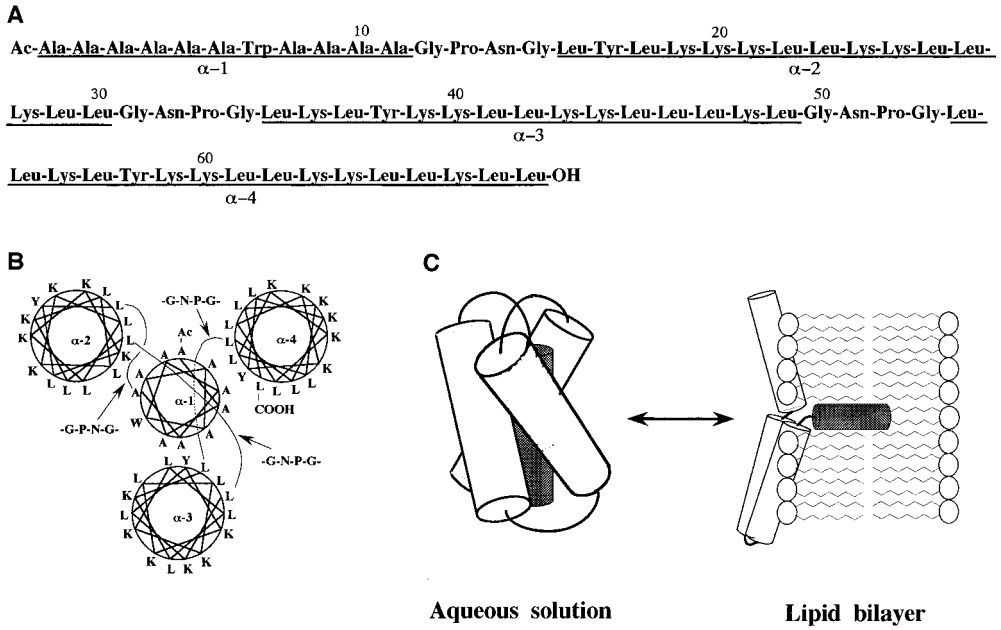

FIGURE 1: Amino acid sequence of SGP (A), helical wheel representation of SGP (B), and a schematic illustration of its expected folding state and open umbrella state in buffer and in membrane, respectively (C).

Thus, the membrane current was measured and recorded as described previously (Agawa et al., 1991).

RESULTS

Design of Small Globular Protein. SGP consists of 69 amino acid residues divided over 4 helical parts: 3 basic amphiphilic helices composed of Leu and Lys and a hydrophobic helix composed of oligoalanine in the middle. Leu, Lys, and Ala have a strong helix-forming potential in globular proteins (Chou & Fasman, 1978). The appropriate periodical distribution of Leu and Lys along chains can induce a stable amphiphilic helical structure at apolar surfaces such as air, the hydrophobic sites of protein, and the phospholipid membrane (DeGrado & Lear, 1985; Blondelle & Houghten, 1992; Kiyota et al., 1996). Oligoalanine (n = 10) was selected as the hydrophobic central helix, which is the smallest in size and shorter in chain length than the other three helices (n = 15). The three helices composed of Lys and Leu residues take on amphiphilic structure when represented as α-helical wheels (Figure 1B). It seems that the three amphiphilic helices can surround smoothly the small hydrophobic central helix. To look at the folding structures, one Trp was introduced in the hydrophobic helix and one Tyr in each amphiphilic helix; the Tyr residue in α-2 is located in the hydrophobic region of the amphiphilic helix and the two Tyr in α-3 and α-4 are located in hydrophobic ones. The α-1 and α-2 helices were connected by a β-turn-forming sequence, Gly-Pro-Asn-Gly to tightly fold and for connections between the other helices (α-2 and α-3, α-3 and α-4); a β-turn-unfavorable one, Gly-Asn-Pro-Gly, was employed to afford flexibility for bending as needed (Chou & Fasman, 1978). In aqueous solution, SGP is expected to take a globular protein-like structure as shown in Figure 1C.

Monomeric State. To demonstrate whether SGP is monomeric or oligomeric in buffer solution, size-exclusion chromatography was performed using a packed column for HPLC (Figure 2). Several natural proteins, known to form compact globular structures, were used as calibration standards. SGP was eluted as a single peak with some tailing

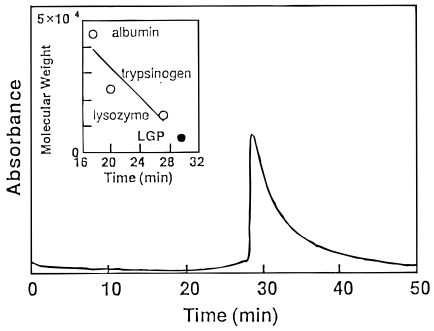

FIGURE 2: Elution profile of SGP on gel-filtration HPLC. SGP was chromatographed on COSMOSIL 5DIOL-300 (Nakarai Tesk, Kyoto, Japan) in 10 mM Tris·HCl, 150 mM NaCl at pH 5.0. Molecular size markers are albumin (45 kDa), trypsinogen (24 kDa), and lyzozyme (14.3 kDa). Inset: molecular weights of the markers (open circles) and SGP (closed circle) were plotted as a function of retention time.

from the gel filtration column. The elution behavior did not change at pH 5.0 and pH 7.4. The tailing seems to be due to partial adsorption of the cationic SGP to the slightly anionic column. The location of this peak is consistent with the expected molecular mass of this protein, indicating that it is monomeric.

Molecular size can also be evaluated by the fluorescence anisotropy and lifetime using Perrin and Einstein−Stokes equations which describe the relationships between the fluorescence anisotropy (r) and the rotational correlation time of the fluorophore (φ) ($r_0/r = 1 + \tau/\varphi$: r_0, intrinsic anisotropy) and between the correlation time and the molecular weight (M) ($\varphi = \eta M\sigma/kT$: η, viscosity; σ, hydration constant; k, Bolzmann constant; T, temperature), respectively (Tao, 1969). The fluorescence anisotropy was decided experimentally as 0.04 in the buffer solution (5 mM Tes, 100 mM NaCl, pH 7.4) (data not shown), and τ was obtained from the decay experiment described later (Table 1), and then the calculated molecular weight is about 6200, indicating that the SGP is monomeric.

This is also supported from analytical ultracentrifugation experiments using a Beckman XLA-TG-2 analytical ultra-

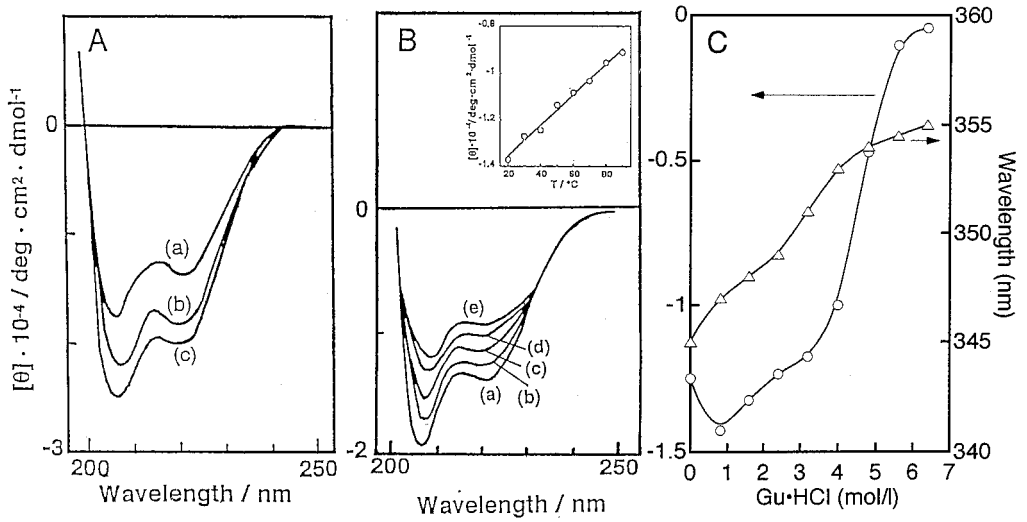

FIGURE 3: Circular dichroism and Trp fluorescence behavior of LPG at different conditions. (A) CD spectra of the peptide in trifluoroethanol (c) buffer (5 mM Tes•HCl and 100 mM NaCl at pH 7.4)(a) and in the presence of egg PC liposomes (b). (B) Temperature dependence of CD spectra in Tes buffer. Peptide concentration, 10 μM. Curves (°C): a, 20; b, 40; c, 60; d, 80; e, 90. (C) Gu•HCl denaturation profiles at 25 °C plotted on the basis of the ellipticity at 222 nm (circles, left *y*-axis) and the emission maximum of Trp fluorescence excited at 285 nm (triangles, right *y*-axis). Peptide concentration is 10 μM.

centrifuge at 60 000 rpm, 20 °C, in 5 mM Tes, 100 mM NaCl, pH 7.4 (data not shown). The data were analyzed by using the XLAEQ program algorithm, and the molecular weight (*M*) was calculated from the following equation: M_b (molecular buoyant) = $M(1 - \upsilon\rho)$. The values of 0.75 and 1 were used as υ (partial specific volume of the particle) and ρ (density of the solvent), respectively. The observed molecular weight is about 7600 at a concentration of about 50 μM.

Spectroscopic Study in Buffer Solution. The conformations of SGP were studied by ultraviolet CD spectroscopic methods (Figure 3A). The dichroic spectrum in 80% trifluoroethanol exhibits negative minima at 206 and 222 nm, characteristic of α-helical structure. In buffer solution, SGP also has a significant content (50%) of helical residues (Chen et al., 1974; Chang et al., 1978). The ellipticities of CD curves of SGP were independent of protein concentrations from 50 μM to 5 μM in buffer solution (data not shown), indicating that no aggregation took place. Interestingly, the presence of egg PC liposomes increased the helical content to 60%.

To understand the stability of SGP, CD and fluorescence spectra were measured as functions of temperature and of guanidine hydrochloride (Gu•HCl) concentration (Figure 3B,C, respectively). The intensities of the minimum trough at 222 nm were decreased linearly with increasing temperatures in the range of 20−90 °C. However, 100% unfolding was not observed even at 90 °C, at which the α-helical content is 35%. The denaturation study using Gu•HCl demonstrated that at low concentration of Gu•HCl at 25 °C, the α-helical content slightly increased when compared with buffer solution only; a similar trend has been observed for molten globular proteins (Goto & Aimoto, 1991). However with increasing concentration, unfolding started at about 4 M Gu•HCl and was complete at 6 M Gu•HCl (Figure 3C). From the smooth cooperative sigmoidal curve obtained, the free energy change (ΔG) was calculated to be 2.5 kcal/mol (Hecht et al., 1990). This value is low relative to water-soluble natural proteins such as lactalbumin (ΔG = 4.2 kcal/mol) and to *de novo* designed four helix bundle proteins (ΔG = 3.7−4.4 kcal/mol) (Regan & DeGrado, 1988) but is comparable to values observed for active destabilized mutant enzymes or betadoublet protein (Quinn et al., 1994). The emission maxima of Trp fluorescence shifted gradually to red wavelength with increasing concentration of Gu•HCl. A relatively strong change was observed in the range of 3−5 M Gu•HCl (Figure 3C), suggesting that the brief conformational change around the Trp residue starts just before the commencement of unfolding of the α-helical structure.

To probe the degree of order in the SGP, binding of the fluorescent dye 1-anilinonaphthalene-8-sulfonate (ANS) was measured. ANS binds strongly to the accessible hydrophobic moiety in molten globular folding structures and to either native or denatured proteins (Semisotnov et al., 1991). The fluorescence of ANS was indeed enhanced by the solution containing SGP (Figure 4A), indicating that binding took place. The dissociation constant and number of binding sites of the SGP−ANS complex evaluated from the increase of the ANS fluorescence intensities are 1.8×10^{-5} M and 1.17, respectively (Wang & Edelman, 1971). Two reasons, *i.e.*, the reduction in the dissociation constant value by 1 order of magnitude as compared with other proteins in the molten globular state ($\sim 10^{-4}$ M) and the presence of a stable, singular hydrophobic binding pocket (only one), suggest that SGP may not be in a molten globular state but somehow in a state similar to a native-like protein (Semisotnov et al., 1991).

Energy Transfer from Tyr to Trp. All of the data support that SGP takes a stable folding structure in the monomeric state. To ascertain whether SGP takes such an expected folding structure as shown in Figure 1C, we measured resonance energy transfer between a Trp in α-1 and one or two of the Tyr in α-2, -3, or -4. The fluorescence decay kinetics of the Trp residue, which were the energy acceptor, were precisely decided using the time-resolved photon counting method. Figure 4B shows the fluorescence decay profile of the Trp residue in SGP in the buffer solution on excitation at 285 nm. According to the general rule of excitation energy transfer kinetics, the fluorescence decay curve of the acceptor molecule must have a truncated form, and its decay kinetics include a negative preexponential factor

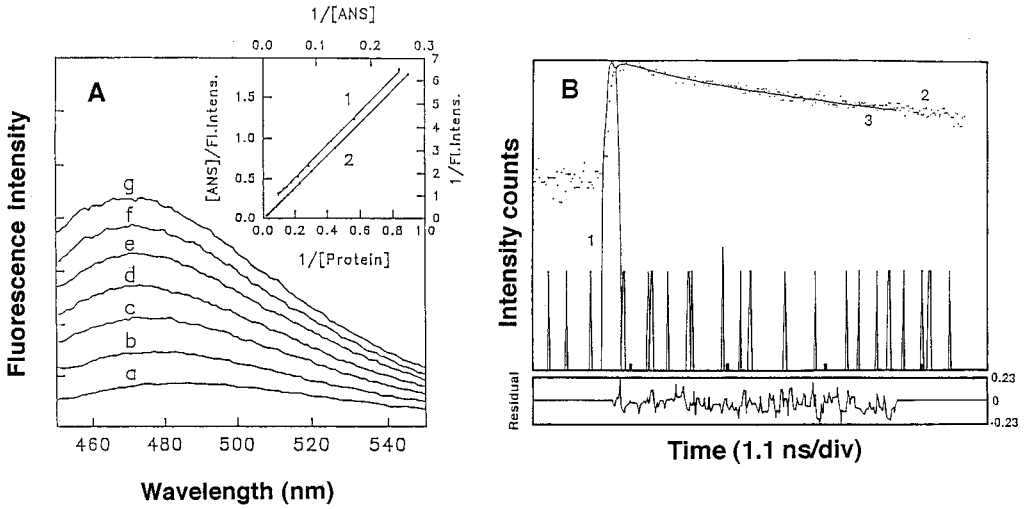

FIGURE 4: (A) Fluorescence emission spectra of ANS bound to SGP. 4 μM ANS was titrated with SGP in 10 mM Tes·HCl at pH 7.4 without changing its concentration. Curves a, b, c, d, e, f, and g include 2.2, 5.5, 8.7, 11.7, 14.7, 17.6, and 20.5 μM SGP, respectively. The excitation wavelength was 370 nm. Insert: estimation of the number of binding sites (n) and dissociation constants (K_d) of SGP against ANS (Eftink & Ghiron, 1976). K_d and n were estimated using eqs 1 and 2: $1/I = 1/I_{max} + (K_d/I_{max})/[ANS]$ is eq 1, and $[ANS]/I = 1/\phi + (K_d/\phi n)/[SGP]$ is eq 2, where I and ϕ are the fluorescence intensity of ANS and the specific fluorescence intensity of bound ANS. I_{max} is the fluorescence intensity of ANS when SGP is saturated with ANS. Line 1 was plotted based on eq 1, titrating 2 μM SGP with ANS (x- and y-axes are given at the upper and right side, respectively). Line 2 was based on eq 2 and obtained with titration of 4 μM ANS with SGP (x- and y-axes are given at the bottom and left side, respectively). (B) Fluorescence decay profile of the Trp residue in 5 mM Tes buffer (pH 7.4) (upper panel). Excitation wavelength, 285 nm; emission wavelength, 350 nm. Total counts are 12 500. Curves 1, 2, and 3 are the excitation pulse, the fluorescence decay profile, and the theoretical curve calculated using the decay parameters giving the best fit. The weighted residuals are shown in the bottom panel.

Table 1: Fluorescence Decay Parameters of SGP[a]

	τ_1 (ps)[b]	τ_2 (ps)	τ_3 (ns)	α_1	α_2	α_3	χ
buffer	53	620	3.3	−0.55	0.63	0.91	1.134
liposome		338	3.40		0.34	0.66	1.005

[a] Excitation wavelength at 285 nm and emission wavelength at 350 nm. [b] The fluorescence decay kinetics were given by a linear combination of exponentials: $F(t) = \sum\alpha_i \exp(-t/\tau_i)$, where α_i and τ_i are the fluorescence lifetime of the ith component and the corresponding preexponential function, respectively.

as shown by eq 1 when the donor molecule is excited:

$$[A^*] = \{k_T[D^*]_0/(1/\tau_A - 1/\tau_D)\} \exp(-t/\tau_D) + \{[A^*]_0 - k_T[D^*]_0/(1/\tau_A - 1/\tau_0)\} \exp(-t/\tau_A) \quad (1)$$

where $[D^*]_0$ and $[A^*]_0$ are the concentrations of excited donor molecules and directly excited acceptor molecules at the instant of excitation, respectively, τ_D and τ_A are decay times of the donor and acceptor, respectively, and k_T is the energy transfer rate constant. The decay profile in buffer solution gave a somewhat truncated form on the initiation of excitation as seen in Figure 4B. The nonlinear deconvolution analysis of the decay profile gave clearer evidence for the excitation energy transfer from Tyr to Trp in the buffer. The fluorescence decay parameters of SGP monitored and excited at 350 and 285 nm, respectively, are summarized in Table 1. The fluorescence of the Trp residue decayed with triple-exponential kinetics in the buffer, and the preexponential factor corresponding to the fastest decay component was negative. On the other hand, the decay profile of the Trp residue in the egg PC liposome membrane rose steeply (data not shown). The fluorescence decay kinetics in the liposome membrane were described definitely with a double exponential with two positive preexponential factors. These results suggest that SGP takes a conformation enabling energy transfer from Tyr to the Trp residue only in the buffer but not in membrane. Unfortunately the intrinsic Tyr's lifetime cannot be measured because of the presence of the energy acceptor (Trp), so it is difficult to estimate the precise energy transfer rate or the efficiency between Tyr and Trp in SGP in the buffer solution. However, the donor's lifetime (τ_1) of SGP was evaluated to be about 53 ps (Table 1). This lifetime is much shorter than the usual fluorescence lifetime of Tyr (about 500 ps to ~2 ns), indicating that the energy transfer of SGP is considerably effective in the buffer solution (Willis & Szabo, 1991). This strongly demonstrates that α-1 associates with the other one or two α-helical segment(s) by adopting a globular protein structure in buffer. On the other hand, in the presence of liposomes, the folding structure changes to a conformation where three Tyr residues are not present near central helices.

Trp Fluorescence Study in the Presence of Liposomes. Next, to examine the translocation of peptide into membrane, the intrinsic fluorescence of Trp was measured in buffer solution and in the presence of liposomes (Figure 5A). When placed in buffer, the peptide exhibited an emission maximum at 345 nm (excited at 290 nm), indicating a less hydrophilic environment for the Trp, because the Trp exposed to a hydrophilic environment usually has an emission maximum around 355 nm (Eftink & Ghiron, 1976). However, with increasing concentration of egg PC liposome, the peptide exhibited an enhanced increment in its fluorescence intensity and a blue shift to 338 nm in the fluorescence emission maximum. Since the fluorescence change reflects relocation of the Trp into a more hydrophobic environment, such a view is not inconsistent with the fluorescence quenching experiments (Figure 5B). The fluorescence intensity decreased with increasing concentration of acrylamide. The quenching data were analyzed according to the Stern−Volmer relationship. The plots in the absence and presence of egg PC gave a straight line, and the slope in the presence of egg PC liposomes (K_{sv} = 5.8 M^{-1}) was smaller than that in the

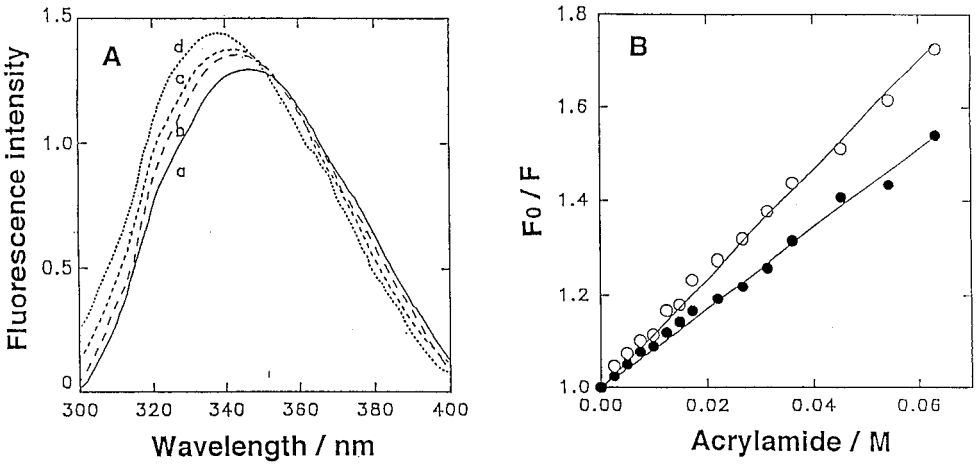

FIGURE 5: (A) Trp fluorescence titration curves for binding of SGP to liposomes as a function of egg PC liposome concentrations. Peptide concentration is 5.2 μM. Lipid concentrations (μM): a, 5; b, 10; c, 20; d, 40. (B) Fluorescence quenching of SGP by acrylamide in the various conditions. The solid lines were obtained with the linear least-squares method. The open circles are in buffer solution, and the closed circles are in the presence of egg PC liposomes.

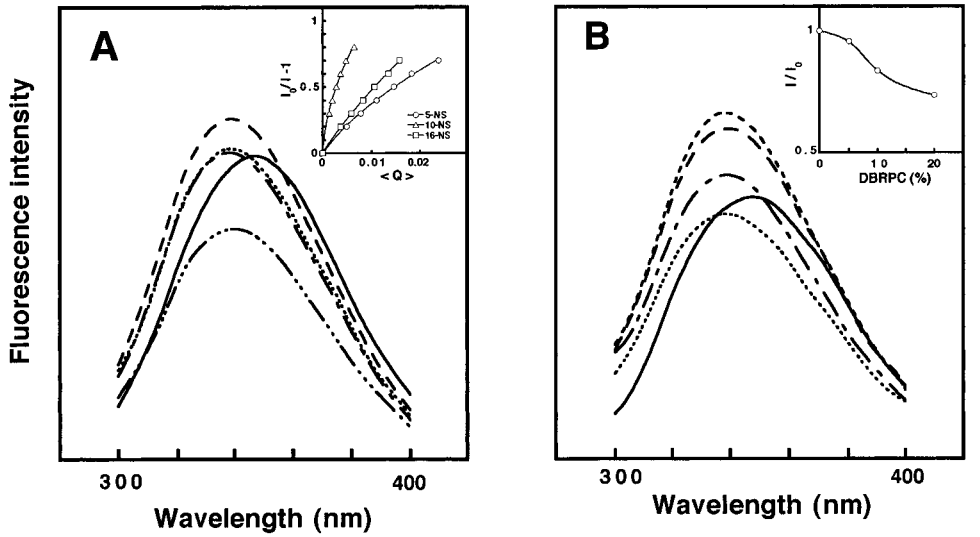

FIGURE 6: (A) Quenching of Trp fluorescence by various *n*-doxylstearic acids in the presence of egg PC liposomes at 25 °C. Peptide (5 μM) was added to egg PC liposome (100 μM) solution containing 4% *n*-doxylstearic acids, 5 mM Tes, and 100 mM NaCl. Buffer (—), egg PC only (— —), 5-NS (···), 10-NS (— · —), and 16-NS (— ··· —). Inset in (A): Titration curves with egg PC liposomes containing *n*-doxylstearic acids. The ratio of the fluorescence maximum intensity (excitation at 290 nm) in the absence of quencher, F_0, to the intensity in the presence of quencher, F, is plotted as a function of the amount of membrane-bound quencher per lipid, $\langle Q \rangle$ (Blatt & Soyer, 1985). (B) Quenching of Trp fluorescence by egg PC liposomes containing different concentrations of DBRPC at 25 °C. Buffer (—), 0% DBPRC (- - -), 5% (— —), 10% (— · —), and 20% (···). Peptide concentration is 5 μM. Lipid concentration is 200 μM.

absence of egg PC liposomes ($K_{sv} = 6.2\ M^{-1}$). The Stern–Volmer constants (K_{sv}) observed tell us that Trp residues both in buffer and in the lipid bilayer are present at the intermediate area between the hydrophilic surface and the hydrophobic interior in molecules or in lipid bilayers (Eftink & Ghiron, 1976).

Depth-Dependent Fluorescent Quenching of Trp in the Presence of Liposomes. To collect detailed information on the position of the helices within the lipid bilayers, the quenching behavior of *n*-doxylstearic acids in egg PC vesicles was investigated (Figure 6A) (Voges et al., 1987). Depth-dependent fluorescent quenching of a Trp located at the hydrophobic helices was checked using a set of *n*-doxylstearic acids ($n = 5, 10, 16$). The *n*-stearic acid bearing the nitroxide label at position 10 (10-NS) incorporated into egg PC liposomes drastically quenched the Trp fluorophore, but 5-NS and 16-NS did weakly. Then, the quenching efficiency of *n*-doxylstearic acid was also compared with the membrane-bound quencher per lipid molecule because the series of *n*-doxylstearic acids differ in the affinity of lipid membranes (Blatt & Soyer, 1985). So, a titrating study of the peptide by *n*-doxylstearic acids incorporated into the outer layer of egg PC liposomes was performed at several lipid concentrations; the results showed that the quenching efficiency is in the order 10-NS $\gg$ 16-NS $\geq$ 5-NS (inset in Figure 6A). From these fluorescence experiments, we concluded that the central helix is localized in lipid bilayers perpendicularly, in which the Trp residue is present at an intermediate depth of lipid core at the outer layer of lipid bilayers, while the three amphiphilic helices may be left at the lipid surface, horizontally. This conclusion was also confirmed from the quenching experiment using the lipid bilayers containing 9,10-DBRPC. As shown in Figure 6B, the fluorescence quenching caused by bromines attached to the 9,10 positions of the twin acyl chains of phospholipid was gradually increased with increasing content of DBRPC

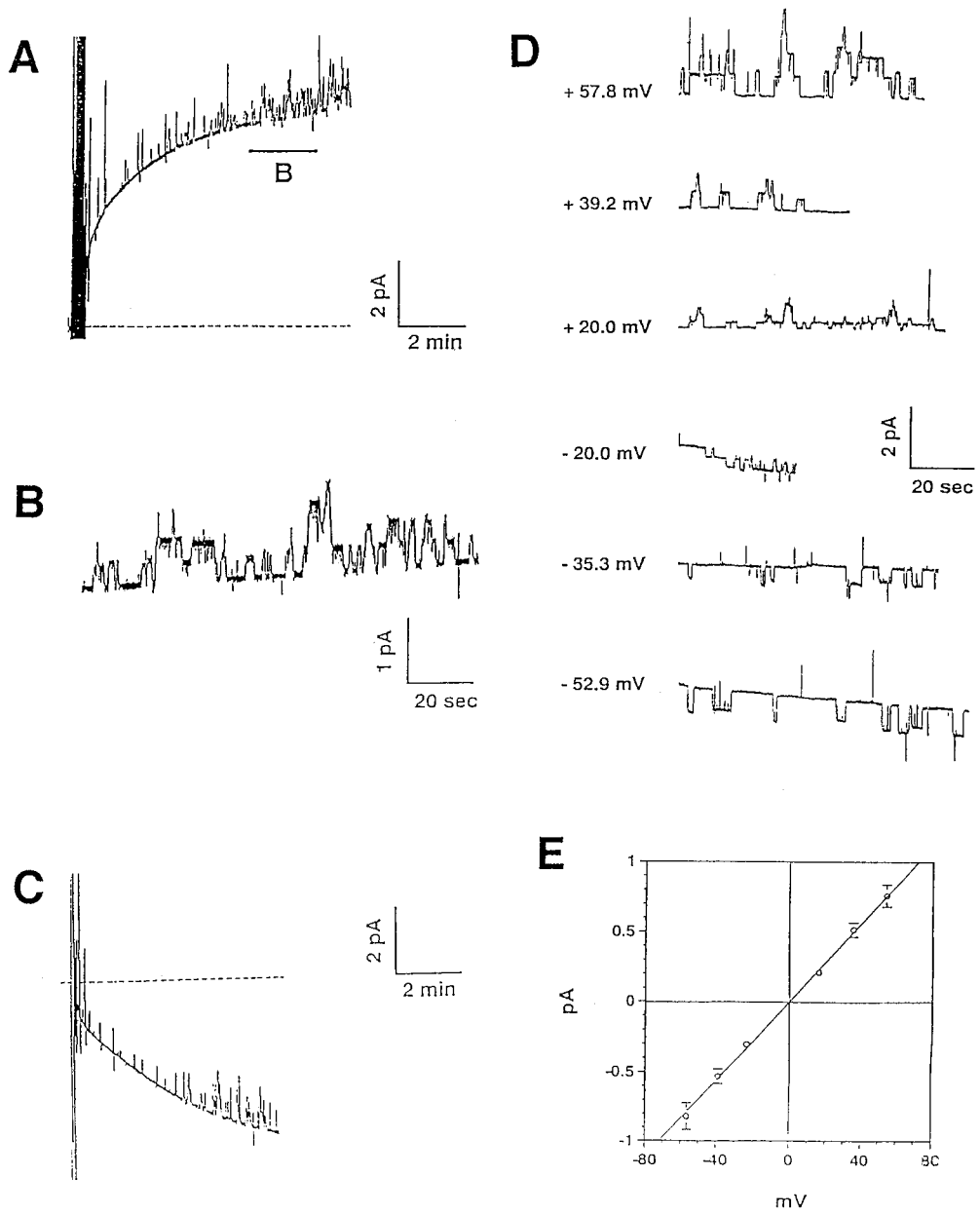

FIGURE 7: Electric current profiles of a bilayer membrane holding SGP. (A) Effect of SGP on the conductance of a planar bilayer membrane. The bilayer was formed by the folding method using egg PE/brain PS (2:1) in symmetrical 1 M KCl and 10 mM Tris−Hepes (pH 7.4). 5 μL of a methanol solution of SGP (1 mg/mL) was added to the cis compartment and stirred for 5−10 s. The trace was filtered at 20 Hz. The membrane potential was kept at +18.5 mV. The dashed line indicates the zero current level. (B) A part of the current trace from panel A. The part of the Figure 7 trace indicated as B was expanded. Filter: 20 Hz. (C) Effect of SGP on the conductance of a planer bilayer membrane in asymmetrical KCl concentration (cis, 600 mM; trans, 150 mM). 5 μL of a methanol solution of SGP (1 mg/mL) was added to the cis compartment. The membrane potentials were kept at almost zero (−0.4 mV). (D) Voltage dependency of the channel events in symmetrical 150 mM KCl and 10 mM Tris−Hepes solution (pH 7.4). (E) Current−potential relationship of the single channel current shown in panel B. From the slope of the graph, the single channel conductance was calculated as 14 pS.

in egg PC liposomes. SGP undergoes a conformational change that results in transferring the Trp position from the protein interior to the area near the 9,10 positions of the phospholipid acyl chain.

Ion Channel Formation. Finally, the planar bilayer method (Montal & Mueller, 1972) was employed to further examine whether the peptide is able to move into the lipid bilayers and to increase the membrane permeability by forming something like an ion channel. When the methanol solution of SGP was added, the membrane current was rapidly increased at first, and the rate of the increase was gradually slowed down (Figure 7A). Here, the current is referred to as basal current. After the basal current reached a certain level, discrete current changes corresponding to channel-event appeared overlapping the basal current. The channels increased in multiples of the single channel level (Figure 7B) with time at the later part of the trace of Figure 7A. When the same amount of SGP dissolved in 150 mM KCl and 10 mM Tris−Hepes (pH 7.4) was added, a similar time course of the current increase was observed (data not shown), suggesting that membrane currents by SGP are not dependent on the structure in the solubilized conditions such as the organic and the aqueous solution. When the concentration of KCl was asymmetrical (cis, 600 mM; trans, 150 mM), SGP also induced two types of membrane currents (basal current and channel current) at almost zero membrane

potential (Figure 7C). Interestingly, the ion selectivity of the basal current and channel events is different. Although no exact ion selectivity of both currents was determined yet, it is likely that the basal current is a little anion-selective while the channel event is cation-selective. The property of the channel current was examined further. Figure 7D demonstrates that the single channel current is dependent on the membrane potential. The current−potential plot ($I-V$ plot in Figure 7E) shows that the single channel conductance is 14 pS at symmetrical 150 mM KCl. The conductance at 1 M KCl is about 17 pS. The conductance at KCl concentrations suggests that the K^+ conductivity of the channel is considerably saturated at 150 mM KCl.

DISCUSSION

The hydrophobic effect is a primary factor to the folding and stabilization of protein structure (Kauzman et al., 1959). Hydrophobic residues tend to cluster into the solvent-inaccessible interiors of globular proteins while hydrophilic residues tend to project outward and are more solvated (Janin, 1979). First of all, it is essential to determine whether SGP is monomeric or oligomeric in buffer solution, because a large hydrophobic part of oligoalanine that may self-assemble is present in the molecule. The present size-exclusion chromatography and the fluorescence anisotropy−lifetime correlation studies as well as the CD measurements indicated that SGP is monomeric with α-helical structure. Analytical ultracentrifugation also demonstrates that SGP is monomeric in the buffer solution. The binding of a hydrophobic dye, ANS, to SGP in buffer solution showed that SGP takes a stable folding structure and possesses a hydrophobic binding site. Moreover, the maximam wavelength of the Trp fluorescence at 345 nm showed that the Trp of the central helix is present at a relatively hydrophobic region. Moreover, the energy transfer experiments showed that the Trp accepts the energy from tyrosines in the other amphiphilic helices, indicating that the hydrophobic alanine oligomer helix is close to one or two other helices. All of these experimental results reveal that SGP takes a stable globular-like structure in aqueous solution. Therefore, it would be expected that the hydrophobic helix of SGP is located to make a hydrophobic core in the central part of the protein as the hydrophobic core is surrounded by amphiphilic helices; the hydrophobic parts of the amphiphilic helices are in contact with the hydrophobic central core while hydrophilic parts are in the solvent-exposed state, resulting in a globular protein (Figure 1B,C).

De novo designed proteins are known to exhibit some of the features of the molten globule, such as marginal stability, low cooperativity of unfolding, ANS binding, and poor NMR resolution characteristics (Regan & DeGrado, 1988; Semisotnov et al., 1990; Kamteker et al., 1993; Quinn et al. 1994; Releigh et al., 1995). Biophysical analyses of *de novo* designed helix−bundle proteins with four amphiphilic α-helices have shown that they are more stable than natural proteins but lack a well-ordered interior, as seen in the molten globule (DeGrado et al., 1988; Lutgring & Chmielewski, 1994). SGP did not completely denature even at high temperature (90 °C) and at relatively high Gu·HCl concentration; the denaturant concentration at the midpoint of the transition is 5 M. These results indicate that SGP exhibits characteristics associated with the molten globular state. However, it should be mentioned that from CD and fluorescence study by the addition of Gu·HCl in buffer solution, SGP is denatured highly cooperatively, and the Trp residue present in the relatively hydrophobic surrounding is exposed to the solution prior to denaturation of the α-helical structure (Figure 3C). Also, the titration study with ANS showed that SGP has one hydrophobic binding site of ANS in the molecules with a dissociation constant on the order of 20 μM. These results indicate that the molten globular-like structure has an aspect of certain native globular-like structures.

The CD data of SGP in buffer solution showed 50% helical content. Assuming that the central oligoalanine residues take a fully α-helical structure, it amounts to about 15% of the total structure. The remaining helical content of the three amphiphilic helices totals up to 35%. This corresponds to the idea of 6−7 of 15 residues of each amphiphilic helical segment. Thus, we image a cationic micelle-like bundle as the structural feature of SGP; that is, the small central α-helical cylinder composed of polyalanine (10 residues) and 1 Trp is surrounded by the partially collapsed 3 larger cylinders composed of Leu and Lys (15 residues/each cylinder), in which Lys residues are scattered to the outer surface by the repulsion of negatively charged groups.

Interestingly, the micelle-like stable structure imaged as described above is easily broken while the hydrophobic central α-helix is penetrated into the lipid bilayer. The depth-dependent fluorescent studies using *n*-doxyl fatty acids and brominated phospholipid as quenchers indicated that the Trp in the central α-helix is present at about the middle of the alkyl chain in the outer layer of the phospholipid bilayer. Since the Trp is present at the middle of the central α-helix, the acetyl group of the N-terminal may be present around the middle of the bilayer. Three amphiphilic helices may be laid around the lipid surface, because no energy transfer was observed from Tyr to Trp in lipid bilayers. According to a classification of the different lipid-associating helices from the hydrophobic and hydrophilic angles that are defined as a sector formed by hydrophobic residues and hydrophilic residues on the helical wheel, the peptide with a helix angle equal to 180° lies parallel to the membrane surface [see Epand et al. (1995) as a review; Brausseur, 1991; Kiyota et al., 1996]. As the three amphiphilic peptide angles of SGP are about 180°, they may be located at the membrane surface in such a manner. It is interesting that two types of membrane current were induced by SGP. The basic properties such as conductance and ion selectivity are very different between these membrane currents. These data suggest that at least two types of interaction modes are present between SGP and the membrane. The insertion of a central α-helix may induce the basal current on the planar lipid bilayer. As the protein accumulates into the outer layer of lipid bilayers, some protein makes a pore causing channel current (Figure 7B). The insertion mechanism may be similar to those for colicins that spontaneously enter the hydrophobic central helices into the lipid bilayer by taking an open umbrella-like structure, and then making a pore with an inverted umbrella-like structure (van der Goot et al., 1991; Mel et al., 1993).

The model of ion channel formation by a bundle of membrane-spanning α-helices surrounding a central pore has received much support both from molecular neurobiological studies and from studies of channel-forming peptides [for a review, see Sansom (1991)]. We have shown that several

basic amphiphilic α-helical or 3_{10}-helical peptides spanning lipid bilayers can form ion channels, but with multilevel conductance (Agawa et al., 1991; Anzai et al., 1991; Iwata et al., 1994). When Heitz et al. (1982) have tested channel-forming properties of oligoalanines of length $n = 10$, 15, 20, and 24 in lipid bilayers, the shorter peptides ($n = 10$, 15) failed to increase bilayer conductance, but the longer peptides ($n = 20$, 24) formed multilevel conductance channels. Thus, the hydrophobic central helix and the three amphiphilic helices may make channels cooperatively as follows: (1) at first, the central hydrophobic helix is penetrated perpendicularly into lipid bilayers while amphiphilic peptides lie horizontally by immersing the hydrophobic parts of the amphiphilic helices into lipid bilayers (an open umbrella-like conformation as shown in Figure 1C); and then (2) some SGP slip more deeply into the membrane by the aid of membrane potentials and so on. At that time, both the central hydrophobic oligoalanine and the basic amphiphilic peptides of single or multiple molecules cooperatively make a pore. The pore length formed by the hydrophobic and amphiphilic helices would be enough to span lipid bilayers. It should be mentioned that the pore formed by SGP molecule(s) takes a uniform structure, because it is not a multi- but a single-gauge conductance channel. Relating to this insertion is the report that the N-terminal attachment of polyalanine ($n = 10$) to bovine pancreatic trypsin inhibitor, a water-soluble carrier protein, is not incorporated in lipid bilayers (Moll & Thompson, 1994). Since the central helix of SGP has the same number of alanines as the semisynthetic protein, the insertion of SGP into the lipid bilayer is not only attributable to the hydrophobicity of the central part, but also to that of the hydrophobic parts of amphiphilic helices.

The inverse protein folding approach seems to be effective in designing novel proteins (Bowie et al., 1991). The architecture of a small size of polypeptide has facilitated the understanding of protein folding or packing of the hydrophobic core. Theoretical work by Dill and colleagues (Lau & Dill, 1990; Yue & Dill, 1992) has suggested that the folding structure may be generated by 50 or more amino acid residues. Experimental work has also reported that a monomeric 23-residue polypeptide takes defined tertiary structure with a hydrophobic core formed by an amphiphilic α-helix and a β-hairpin (Struthers et al., 1995). Thus, SGP consisting of 69 residues may also be a useful model to construct amino acid sequences that fold to a desired native-like conformation, to select the appropriate location for the hydrophobic and hydrophilic amino acid residues, and to observe space filling of amino acid residues in the protein interior.

The 4-α-helical bundle structure has often been found in natural proteins (Weber & Salemme, 1980). In the accepted steric arrangement, the 4 helices are nearly 4-fold symmetrical, and the interhelix angle is near 18°. Although SGP may contain four packed α-helical segments, the working assumption that it behaves as a 4-symmetrical α-helical structure lies outside the scope of our consideration. Additional chemical, crystallographic, and spectroscopic investigations are necessary to determine the precise arrangement of the helices and whether particular hydrophobic pockets are present in the molecule or not.

There have so far appeared a number of reports that water-soluble toxins from pathogenic bacteria are spontaneously inserted into the membranes of the target cell (Konisky, 1982). Their insertion is often accompanied by channel formation. SGP was also spontaneously inserted into lipid bilayers, resulting in forming the channels. Interestingly, SGP exhibited strong hemolytic activity but not antimicrobial activity (data not shown). SGP may be a basic and starting model to search translocation mechanisms of the water-soluble toxins from aqueous solution into lipid bilayers.

ACKNOWLEDGMENT

We thank Dr. H. Hanazono, Fukuoka University, for the FAB mass spectral measurement. We are grateful to Dr. T. Koga and Dr. A. Takase, National Institute for Industrial Technology in Kyushu, for the measurements of the fluorescence decay.

REFERENCES

Agawa, Y., Lee, S., Ono, S., Aoyagi, H., Ohno, M., Taniguchi, T., Anzai, K., & Kirino, Y. (1991) *J. Biol. Chem. 266*, 20218−20222.

Anzai, K., Hamasuna, M., Kadono, H., Lee, S., Aoyagi, H., & Kirino, Y. (1991) *Biochim. Biophys. Acta 1064*, 256−266.

Blatt, E., & Soyer, W. H. (1985) *Biochim. Biophys. Acta 896*, 64−76.

Bloudelle, S. E., & Houghten, R. A. (1992) *Biochemistry 31*, 12688−12694.

Bowie, J. U., Lüthy, R., & Eisenberg, D. (1991) *Science 253*, 164−170.

Brausseur, R. (1991) *J. Biol. Chem. 226*, 16120−16127.

Bryson, J. W., Betz, S. F., Lu, H. S., Suich, D. J., Zhou, H. X., O'Neil, K. T., & DeGrado, W. F. (1995) *Science 27*, 935−941.

Chang, C. T., Wu, C.-S. C., & Yang, J. T. (1978) *Anal. Chem. 91*, 13−31.

Chen, Y.-H., Yang, J. T., & Chau, K. H. (1974) *Biochemistry 13*, 3350−3359.

Chou, P. Y., & Fasman, G. D. (1978) *Annu. Rev. Biochem. 47*, 251−276.

Dawidowicz, E. A., & Rothman, J. E. (1976) *Biochim. Biophys. Acta 455*, 621−630.

DeGrado, W. F., Wasserman, Z. R., & Lear, J. D. (1989) *Science 243*, 622−628.

Dekker, N., Cox, M., Boelens, R., Verrijzer, C. P., van der Vliet, P. C., & Kaptein, R. (1993) *Nature 362*, 852−855.

Eftink, M. R., & Ghiron, C. A. (1976) *Biochemistry 15*, 672−680.

Epand, R. M., Shai, Y., Segrest, J. P., & Anantharamaiah, G. M. (1995) *Biopolymers 37*, 319−338.

Goto, Y., & Aimoto, S. (1991) *J. Mol. Biol. 218*, 387−396.

Handel, T. M., Williams, S. A., & DeGrado, W. F. (1993) *Science 261*, 879−885.

Hecht, M. H., Richardson, J. S., Richardson, D. C., & Ogden, R. C. (1990) *Science 249*, 884−891.

Heitz, F., Spach, G., Seta, P., & Gavach, C. (1982) *Biochem. Biophys. Res. Commun. 107*, 481−484.

Iwata, T., Lee, S., Oishi, O., Aoyagi, H., Ohno, M., Anzai, K., Kirino, Y., & Sugihara, G. (1994) *J. Biol. Chem. 269*, 4928−4933.

Janin, J. (1979) *Nature 277*, 491−492.

Kamtekar, S., Schiffer, J. M., Xiong, H., Babik, J. M., & Hecht, M. H. (1993) *Science 262*, 1680−1685.

Kauzmann, W. (1959) *Adv. Protein Chem. 14*, 1−46.

Kiyota, T., Lee, S., & Sugihara, G. (1996) *Biochemistry 35*, 13196−13204.

Konisky, J. (1982) *Annu. Rev. Microbiol. 36*, 125−144.

Lau, K. F., & Dill, K. A. (1990) *Proc. Natl. Acad. Sci. U.S.A. 87*, 638−642.

Lutgring, R., & Chmielewski, J. (1994) *J. Am. Chem. Soc. 116*, 6451−6452.

McKinnon, A. E., Szabo, A. G., & Miller, D. (1977) *J. Phys. Chem. 81*, 1564−1570.

Mel, S. F., Falick, A. M., Burlingame, A. L., & Stroud, R. M. (1993) *Biochemistry 32*, 9473−9479.

Moll, T. S., & Thompson, T. E. (1994) *Biochemistry 33*, 15469−15482.
Monera, O. D., Zhou, N. E., Lavigne, P., Kay, C. M., & Hodges, R. S. (1996) *J. Biol. Chem. 271*, 3995−4001.
Montal, M., & Mueller, P. (1972) *Proc. Natl. Acad. Sci. U.S.A. 69*, 3561−3566.
Parker, M. W., Pattus, F., Tucker, A. D., & Tsernoglou, D. (1989) *Nature 337*, 93−96.
Quinn, T. P., Tweedy, N. B., Williams, R. W., Richardson, J. S., & Richardson, D. C. (1994) *Proc. Natl. Acad. Sci. U.S.A. 91*, 8747−8751.
Raleigh, D. P., Betz, S. F., & DeGrado, W. F. (1995) *J. Am. Chem. Soc. 117*, 7558−7559.
Regan, L., & DeGrado, W. F. (1988) *Science 241*, 976−978.
Sansom, M. S. P. (1991) *Prog. Biophys Mol. Biol. 55*, 135−235.
Semisotnov, G. V., Rodionova, N. A., Razgulyaev, O. I., Uversky, V. N., Gripas', A. F., & Gilmanshin, R. I. (1991) *Biopolymers 31*, 119−128.
Struthers, M. D., Cheng, R. P., & Imperiali, B. (1996) *Science 271*, 342−345.
Tao, T. (1969) *Biopolymers 8*, 609−632.
van der Goot, F. G., González-Mañas, J. M., Lakey, J. H., & Pattus, F. (1991) *Nature 354*, 408−410.
Voges, K.-P., Jung, G., & Sawyer, W. H. (1987) *Biochim. Biophys. Acta 896*, 64−76.
Wang, J. L., & Edelman, G. M. (1971) *J. Biol. Chem. 246*, 1185−1191.
Weber, P. C., & Salemme, F. R. (1980) *Nature 287*, 82−84.
Willis, K. J., & Szabo, A. G. (1991) *J. Phys. Chem. 95*, 1585−1589.
Yue, K., & Dill, K. A. (1992) *Proc. Natl. Acad. Sci. U.S.A. 89*, 4163−4167.
Zhou, N. E., Kay, C. M., & Hodges, R. S. (1992) *J. Biol. Chem. 267*, 2664−2670.

BI962451V